Available online at www.sciencedirect.com
ScienceDirect
Geochimica et Cosmochimica Acta 71 (2007) 3518–3532
Geochimica et Cosmochimica Acta
www.elsevier.com/locate/gca

Structural environments of carboxyl groups in natural organic molecules from terrestrial systems. Part 1: Infrared spectroscopy

Michael B. Hay [a], Satish C.B. Myneni [b,*]

[a] Department of Civil and Environmental Engineering, Princeton University, Princeton, NJ 08544, USA
[b] Department of Geosciences, Princeton University, 151 Guyot Hall, Princeton, NJ 08544, USA

Received 11 April 2006; accepted in revised form 19 March 2007; available online 8 May 2007

Abstract

Carboxyls play an important role in the chemistry of natural organic molecules (NOM) in the environment, and their behavior is dependent on local structural environment within the macromolecule. We studied the structural environments of carboxyl groups in dissolved NOM from the Pine Barrens (New Jersey, USA), and IHSS NOM isolates from soils and river waters using attenuated total reflection Fourier-transform infrared (ATR-FTIR) spectroscopy. It is well established that the energies of the asymmetric stretching vibrations of the carboxylate anion (COO^-) are sensitive to the structural environment of the carboxyl group. These energies were compiled from previous infrared studies on small organic acids for a wide variety of carboxyl structural environments and compared with the carboxyl spectral features of the NOM samples. We found that the asymmetric stretching peaks for all NOM samples occur within a narrow range centered at 1578 cm^{-1}, suggesting that all NOM samples examined primarily contain very similar carboxyl structures, independent of sample source and isolation techniques employed. The small aliphatic acids containing hydroxyl (e.g., D-lactate, gluconate), ether/ester (methoxyacetate, acetoxyacetate), and carboxylate (malonate) substitutions on the α-carbon, and the aromatic acids salicylate (*ortho*-OH) and furancarboxylate (*O*-heterocycle), exhibit strong overlap with the NOM range, indicating that similar structures may be common in NOM. The width of the asymmetric peak suggests that the structural heterogeneity among the predominant carboxyl configurations in NOM is small. Changes in peak area with pH at energies distant from the peak at 1578 cm^{-1}, however, may be indicative of a small fraction of other aromatic carboxyls and aliphatic structures lacking α-substitution. This information is important in understanding NOM–metal and mineral-surface complexation, and in building appropriate structural and mechanistic models of humic materials.

1. INTRODUCTION

Natural organic molecules (NOM) are key components in the physical, chemical, and biological processes that occur in all ecosystems. In terrestrial environments, NOM are known to play an important role in mineral weathering, metal speciation and transport, nutrient retention, organic and inorganic contaminant mobility, and acid buffering (Sposito, 1989; Stevenson, 1994). Much of the chemical activity of NOM is the result of a high concentration of oxygen, nitrogen, and sulfur containing functional groups. Oxygen, which may be present as carbonyl, carboxylic, alcoholic, and phenolic groups, and as ester and ether linkages, is particularly important due to its high abundance. Several of these forms may act as metal-binding ligands, while phenolic and carboxylic acid groups also serve as important sources of acidity. Carboxyl groups are the most dominant forms of oxygen in NOM and are more acidic than phenolic groups. In many respects, carboxyl groups are the most important functional groups in NOM, accounting for the majority of their charge, acidity, and metal and particle surface binding characteristics (Stevenson,

* Corresponding author.
E-mail address: smyneni@princeton.edu (S.C.B. Myneni).

0016-7037/$ - see front matter © 2007 Elsevier Ltd. All rights reserved.
doi:10.1016/j.gca.2007.03.038

1994). In this paper, the term ''carboxyl group'' is used to refer to both the carboxylic acid and its conjugate base, the ''carboxylate'', and is not applied more generally to include ester functionalities. The term ''carboxylic acid'' may refer to the protonated carboxyl group and to the small chain model organic acid molecules.

Though much is known about the types and relative concentrations of different functional groups in NOM, their roles in the biogeochemical processes mentioned above are often difficult to assess. This is because the chemical behavior of a functional group is dependent on its chemical and structural environment (i.e., the types and positions of atoms within the macromolecule, connected to or in the immediate vicinity of the functional group), which is poorly understood for functional groups in NOM. This is particularly true for carboxyl groups. For example, acidities of carboxylic acids and their metal complexation strengths vary significantly based on the local coordination environment of the carboxyl (Goulden and Scott, 1968; Cabaniss and McVey, 1995; Cabaniss et al., 1998). Molecular configuration also governs the degree to which additional functional groups such as carbonyls and hydroxyls may participate with a carboxyl group in metal chelation, which accounts for the strong metal affinity of many natural organic acids. Chelation reactions may be predicted for several smaller biological molecules, such as simple organic acids (e.g., oxalate, citrate) and siderophores, but the chemical structures of more complex, highly degraded long-chain biomacromolecules are still largely unknown, thereby limiting our understanding of carboxyl group chemistry in NOM.

There is also disagreement in the literature over whether the majority of carboxyl groups in NOM are bound directly to aromatic rings or to aliphatic chains. Early on, work by Schnitzer and co-workers emphasized the importance of aromatic carboxyl groups (e.g., salicylate, phthalate) in fulvic acid (Schnitzer and Skinner, 1965; Schnitzer, 1969; Gamble et al., 1970). Salicylate was proposed in part based on chemical studies suggesting that phenolic OH and the carboxylate anion simultaneously participate in metal chelation, while alcoholic OH does not (Schnitzer and Skinner, 1965). Since then, salicylate has been a particularly popular choice as a general humic substance analogue (for example, see Yost et al., 1990; Stevenson, 1994; Hadzija and Spoljar, 1995; Celi et al., 1997; Kubicki et al., 1997; and Dupuy and Douay, 2001). Aromatic carboxyl groups have also been implicated in the RANDOM modeling studies of Murray and Linder (1983; 1984; Linder and Murray, 1987), in which molecular structures are assembled as random assortments of functional groups within a mixed aromatic/aliphatic polymer matrix. The goal of this model, which uses empirical inputs that include aromaticity and elemental/functional group composition, is to construct reasonable NOM molecular structures based on available experimental results. Both salicylate and phthalate are preferred from the perspective of chelate stability in these modeling studies because the aromatic ring can impart additional rigidity to the complex; such an arrangement cannot be guaranteed with substituted aliphatic groups in large macromolecules (Murray and Linder, 1984). An aromatic acid bias may also be present in many of the proposed structures in the literature. In the RANDOM models, the percentage of aromatic carboxylic acids (an input parameter) was chosen such that aromatic substitution was maximized (Murray and Linder, 1983). Additionally, chemical methods that employ oxidative degradation procedures can disproportionately destroy or alter aliphatic structures (Reuter et al., 1983; Leenheer et al., 1995a), and models based on these results may overestimate the aromatic acid fraction.

Evidence also exists that suggests a predominance of aliphatic carboxylic acids in NOM. Thorn (1989) and Leenheer et al. (1995a) have shown that the aromatic and saturated aliphatic carboxyl signatures are resolved in the ^{13}C NMR spectra of fulvic acid dissolved in dimethyl sulfoxide-d_6 (α/β-unsaturated aliphatic and aromatic carboxyls are indistinguishable). After methylation of the carboxylic acids to reduce interference from quinone and ester carbonyl, the carboxylic composition of Suwannee River fulvic acid was determined to be 22% aromatic/olefinic and 78% aliphatic. Based on model compound studies, 27% of the aliphatic carboxyls (i.e., 21% of the total carboxyl content) were thought to have ether/ester linkages in the α position, likely in the form of oxygen-heterocyclic rings, while 4% (3% of total) have an α-keto substitution, consistent with the highly acidic nature of the fulvic acid (Leenheer et al., 1995a,b, 2003). Similar studies on the isolated ''metal-binding'' fraction of fulvic acid also revealed the presence of succinic and tartronic acid type structures (or similar short-chain, *O*-substituted dicarboxylic acids) bound within the macromolecules that participate in multidentate coordination with metals (Leenheer et al., 1998). Evidence for these structures is also supported by proposed oxidative ring opening reactions during humification (Crawford, 1981; Wershaw et al., 1996; Leenheer et al., 1998). The predominance of aliphatic carboxyls has been suggested by other studies on metal–NOM complexes as well. Based on fulvic acid and model organic ligand interactions with Cu^{2+}, Gregor et al. (1989a,b; Town and Powell, 1993) proposed that substituted aliphatic carboxylic groups, including malonate, citrate, and amino acid/peptide structures, might play an important role in metal chelation.

Regardless of the structural types proposed, all of the observations discussed above suggest that substitutions are necessary in the vicinity (α, β-carbon) of the carboxyl group to explain acidity and metal interactions. Given the relative abundance of oxygen functional groups, the majority of these substitutions are presumably in the form of carbonyl, alcoholic, phenolic or ether/ester substitutions, or adjacent carboxyls. In this study, we used attenuated total reflection Fourier-transform infrared (ATR-FTIR) spectroscopy to probe the structural environment of carboxyl groups in NOM directly without any chemical treatment. Many examples exist in the literature in which infrared spectroscopy has been used as a probe to detect the presence and relative abundance of carboxyl groups in NOM, while some authors have suggested ways in which infrared spectroscopy, with proper calibration, can be used as a method for determining absolute carboxylic concentrations (Cabaniss, 1991; Hadzija and Spoljar, 1995). Though examples exist where infrared spectroscopy was used to infer

carboxyl structural types after chemical treatment (e.g., cyclic anhydride formation (Wood et al., 1961; Wagner and Stevenson, 1965)), to the authors' knowledge, direct inference of carboxyl group structural environments in NOM has not been made from their infrared spectra. In this study, we examined carboxyl group environments in isolated NOM from different sources and pristine fluvial NOM using ATR-FTIR spectroscopy. To aid in the interpretation of our results, a brief discussion on the infrared spectral characteristics of carboxyl groups and how they vary with chemical and structural environment is presented below.

1.1. Infrared spectroscopy of carboxyl groups

Infrared spectroscopy is a useful technique in the selective study of carboxyl groups in both small organic acids and organic macromolecules. The large polarities of the C—O bonds result in high infrared activity, giving rise to strong, characteristic vibrational bands, which vary significantly and predictably with pH. The C—O bonds are dissimilar in a protonated carboxyl group, giving rise to independent vibrational modes for C=O and C—OH (Fig. 1). The absorption maximum corresponding to the stretching mode for C=O ($\nu_{C=O}$) is found between 1690 and 1750 cm^{-1}. The vibrations of the C—OH bond (ν_{C-OH}), comprised of a mixture of C—O stretch and C—O—H bend, are found between 1200 and 1300 cm^{-1}. This latter feature appears broad and its identification is often difficult because of the overlap of bending and stretching modes, a strong degree of H-bonding with solvent molecules, and vibrational coupling with C—C and C—OH (alcohol) (Cabaniss et al., 1998). Upon deprotonation of the carboxylic acid, electron density is shared equally between the two equivalent C—O bonds in the carboxylate anion. The C—O stretching modes of the carboxylate cannot be treated as independent vibrations, but contribute equally to symmetric (ν_s) and asymmetric (ν_{as}) vibrational modes (Fig. 1). Asymmetric stretching frequencies for aqueous carboxylates are typically found between 1540 and 1650 cm^{-1}, while those corresponding to the symmetric stretch are found between 1300 and 1420 cm^{-1} (Pike et al., 1993; Cabaniss and McVey, 1995; Cabaniss et al., 1998). Of these two carboxylate modes, ν_{as} is assumed to be the better diagnostic in this study because ν_{as} is less susceptible to vibrational coupling than ν_s (Bellamy, 1980; Yost et al., 1990; Cabaniss et al., 1998).

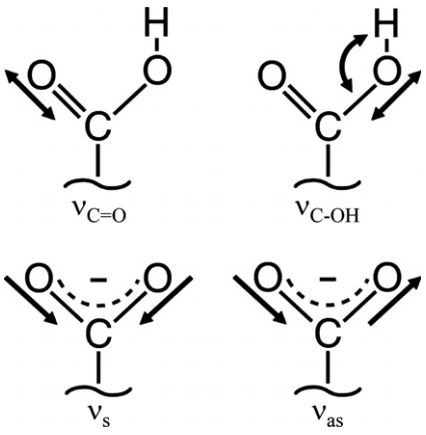

Fig. 1. Vibrational modes of the carboxylic acid and carboxylate anion. The symbols $\nu_{C=O}$, ν_{C-OH}, ν_s, and ν_{as} are used to represent the different vibrations.

A compilation of carboxylate vibrational energies for a variety of smaller aliphatic and aromatic carboxylates is given in Figs. 2 and 3. The carboxylate anion vibrational modes have been chosen over the carboxylic acid vibrations for comparison because of their greater abundance in the literature, proven correlations between ν_{as} and chemical structure, and the complicated behavior of the ν_{C-OH} noted above.

The energies of the carboxylate absorption bands depend on a number of factors, including: (i) electron density on the carboxylic carbon resulting from local molecular structure, (ii) inter- or intramolecular H-bonding involving the carboxylic oxygens and/or the proton in the carboxylic acid, (iii) interactions with metal cations, and (iv) coupling with other vibrational modes in the molecule. In the absence of vibrational coupling, the infrared signature of the carboxylate is directly related to its local structural and chemical environment, and as such, to its chemical behavior. Since vibrational coupling is minimal for ν_{as}, a strong correlation exists between ν_{as} and the chemical behavior of carboxylic acids, as demonstrated by the linear correlation observed between ν_{as} and pK_a (Goulden and Scott, 1968; Cabaniss and McVey, 1995; Cabaniss et al., 1998). The first three factors affecting the vibrational energy of ν_{as} are discussed in detail below.

1.1.1. Effects of electron-withdrawing groups

Electron-withdrawing groups adjacent to a carboxyl group decrease the electron density on the carboxylic carbon, leading to an increase in ν_{as}. The magnitude of the shift is dependent on the electron withdrawing capacity (electronegativity) of the substituent, the number of substituents on the molecule, and their proximity to the carboxyl group (Figs. 2 and 3). For example, in the case of the halogenated acetates, increasing either the number of halogen atoms (chloroacetate → dichloroacetate → trichloroacetate) or the electronegativity of the halogen (iodoacetate → bromoacetate → chloroacetate) on the α-carbon leads to a shift in ν_{as} to higher energy (Spinner, 1964; Cabaniss and McVey, 1995). Strong differences in ν_s are also observed among these molecules, but are less predictable; ν_s increases with increasing electronegativity of the halogen, but decreases with increasing number of halogens (Fig. 4). This opposite trend for ν_s may be the result of changes in the degree of vibrational coupling with varying substituents (Bellamy, 1980; Cabaniss et al., 1998).

A similar trend in ν_{as} is observed for the unsubstituted straight-chain alkyl carboxylates (formate through hexanoate, Fig. 2). The ν_{as} decreases with increasing chain length (or increasing separation between methyl and carboxyl group), approaching an asymptotic value of approximately 1540 cm^{-1}. Each respective decrease in ν_{as} is the result of methyl group substitution on the terminal carbon, and

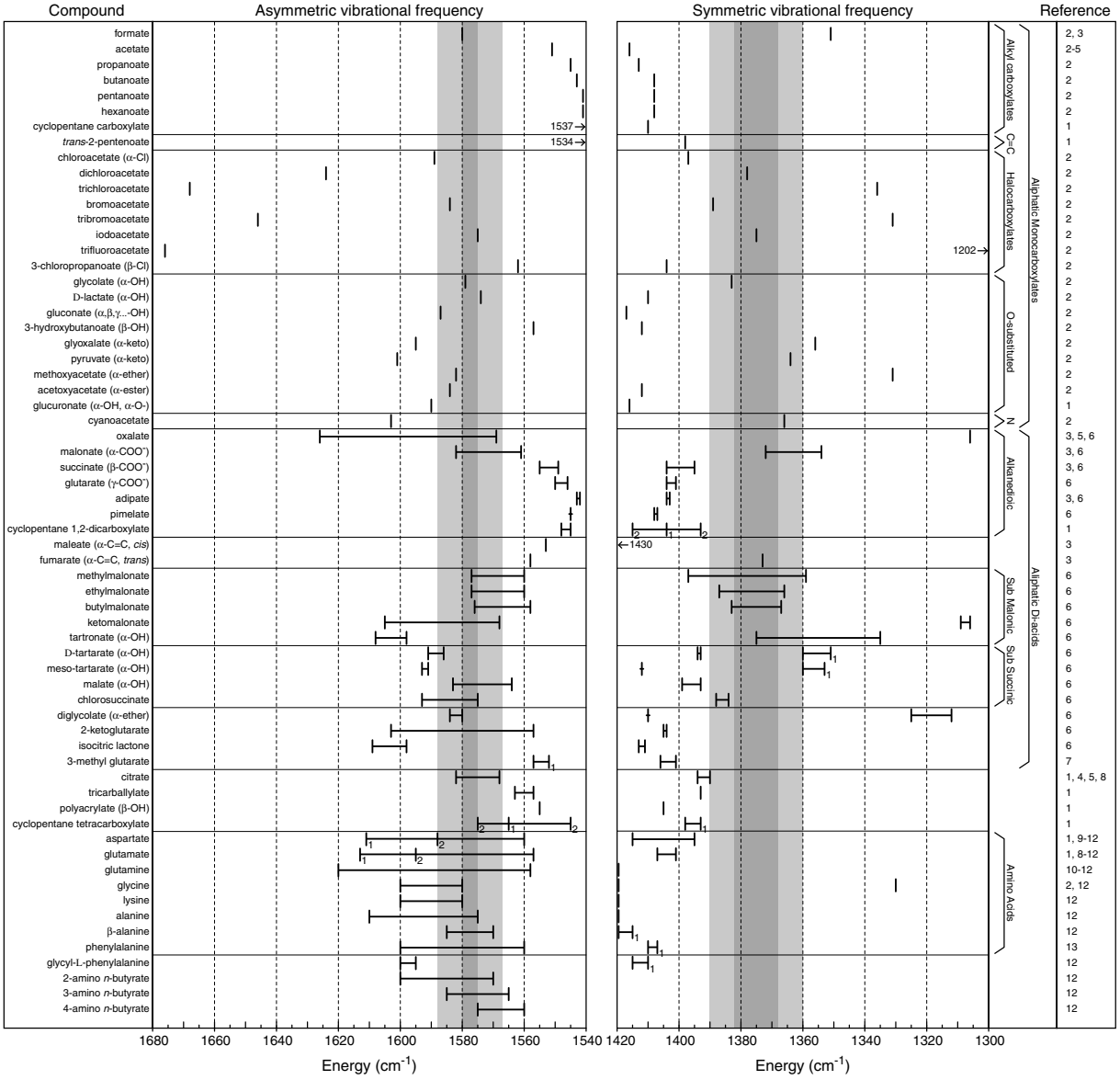

Fig. 2. Asymmetric and symmetric stretching frequencies of aliphatic carboxylates. For polyacids, two or more ν_{as} values are given and are connected by lines. In almost all cases (exceptions noted in the figure with a number), the higher energy peak occurs above the 1st acid pK_a and below the 2nd; after deprotonation of the second carboxylate, the peak shifts to the lower energy. For amino acids and related compounds (aspartate – 4-amino *n* butyrate), the first pK_a corresponds to the carboxyl deprotonation and the second (or third, for aspartate and glutamate) to the amine, and the higher energy peak corresponds to the zwitterion. The dark gray bars represent the range of values found for the natural organics in this study, with a $-10\ cm^{-1}$ correction applied to the ν_{as} to account for drying effects (see text). These regions are extended $\pm 8\ cm^{-1}$ by lighter gray bars to account for uncertainty and heterogeneity. The cyclopentane 1,2-dicarboxylate value is for the *trans* conformation, while all carboxylates in the cyclopentane tetracarboxylate are in the *cis* conformation. Values were compiled from the following: (1) this study, (2) Cabaniss and McVey (1995), (3) Dobson and McQuillan (1999), (4) Katlafsky and Keller (1963), (5) Kubicki et al. (1999), (6) Cabaniss et al. (1998), (7) Roger et al. (2003), (8) Pike et al. (1993), (9) Roddick-Lanzilotta and McQuillan (2000), (10) Barth (2000), (11) Rahmelow et al. (1998), (12) Pearson and Slifkin (1972), and (13) Olsztynska et al. (2001).

the effect of substitution on ν_{as} diminishes with increasing distance from the carboxyl group. It is reasonable to expect the $1540\ cm^{-1}$ limit to be representative of larger alkanes or even more generally, large aliphatic carboxylic acids without a significant degree of substitution in the vicinity of the carboxylate (i.e., lacking substitution on the first few methylene groups). This value is also close to the cyclopentane carboxylate value of $1537\ cm^{-1}$, extending the general result to alicyclic acids and acids located midway through an unsubstituted aliphatic chain. Note that the alkanedioic acids, from oxalate to pimelate, exhibit a similar trend with increasing separation between the carboxyl groups, with the pimelate ν_{as} near $1545\ cm^{-1}$ (Fig. 2). While the changes in ν_s are not as consistent for the alkanoic monoacids, this value also converges with increasing chain length, to a value of $1408\ cm^{-1}$ for both hexanoate and pimelate.

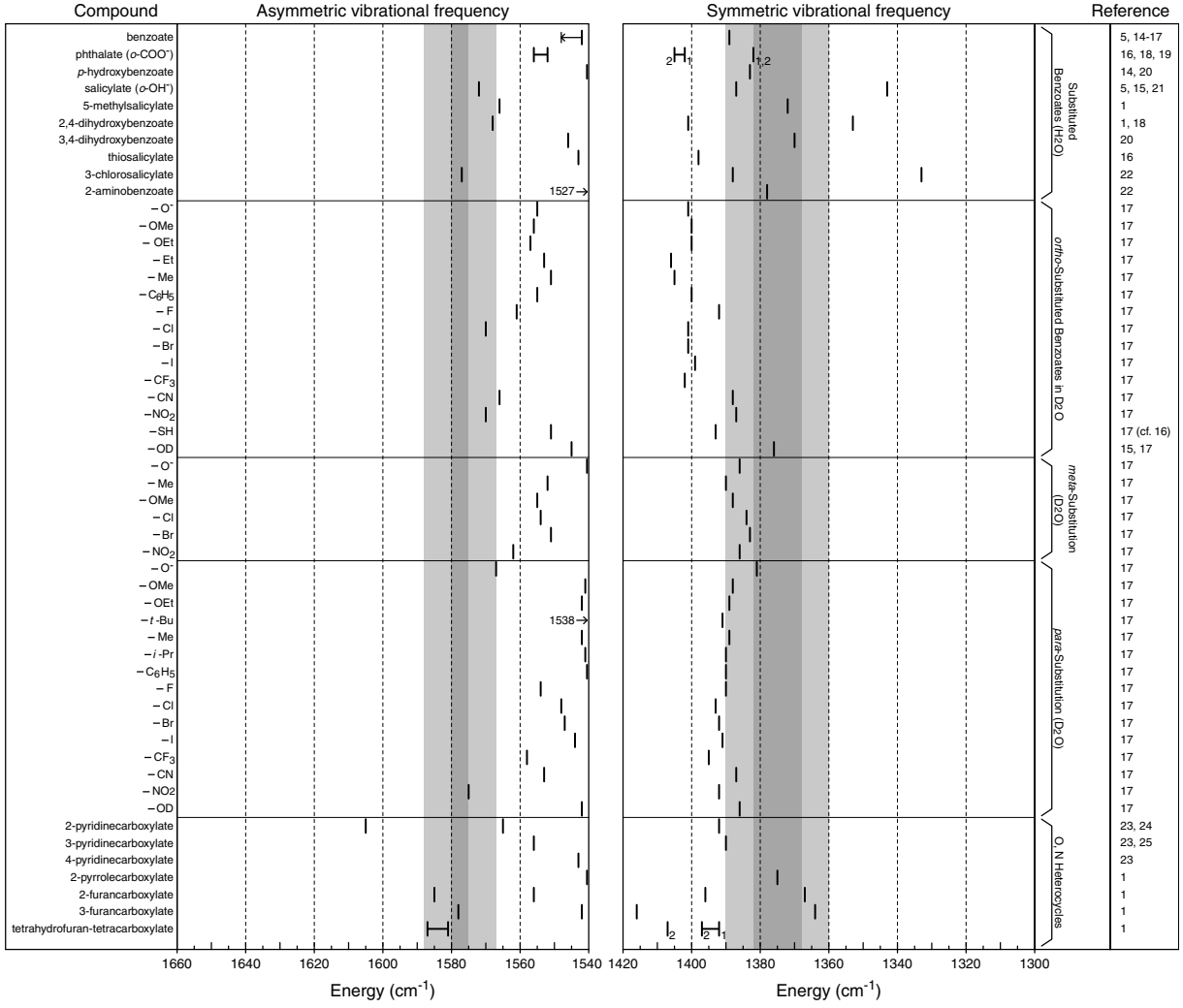

Fig. 3. Asymmetric and symmetric stretching frequencies of aromatic carboxylates (substituted benzoates and heterocyclic compounds). The upper-limit for benzoate indicated by the arrow (1548 cm^{-1}) represents the Dunn and McDonald (1969) value in D_2O. Though the value deviates only slightly from other reported values in H_2O, it may be more useful for comparison with Dunn's other values, assuming internal consistency. In cases where split v_{as} and v_s bands were observed, both values are given. (see Fig. 2 for other details.) Values were compiled from the following: (1) this study, (14) Tejedor-Tejedor et al. (1990), (15) Yost et al. (1990), (16) Dobson and McQuillan (2000), (17) Dunn and McDonald (1969), (18) Tejedor-Tejedor et al. (1992), (19) Loring et al. (2001), (20) Specht and Frimmel (2001), (21) Humbert et al. (1998), (22) Tunesi and Anderson (1992), (23) Wojcik and Stock (1969), (24) Loring et al. (2000), and (25) Wang and Berglund (2000).

Aromatic carboxylates with electron-withdrawing substituents (e.g., substituted benzoates; Fig. 3) also exhibit higher v_{as} values, with trends similar to those noted above for aliphatic compounds. For example, the v_{as} mode of the carboxylate in *para*-halogenated benzoates decreases in the order F > Cl > Br > I. However, the conjugated π electron system in aromatic compounds leads to more complex behavior. In addition to electron withdrawing (inductive) effects, substituents may also contribute electrons to the π electron system, leading to resonance or conjugative effects that are highly dependent on the position of substitution. For example, resonance effects play a strong role in stabilizing the carboxylate anion in 2- and 4-nitrobenzoate, which exhibit higher v_{as} values than 3-nitrobenzoate. Vibrational coupling between v_{as} and ring vibrations may also affect the v_{as} band positions, leading to a poor correlation between v_{as} and acid pK_a for substituted aromatic carboxylates (Dunn and McDonald, 1969). The energies of ring vibrations and the degree of coupling are largely dependent on the type of substitution (Dunn and McDonald, 1969).

In general, the effects of substitution on v_{as} are smaller for the aromatic carboxylates than for the aliphatic compounds. Since the nearest possible substitution in aromatic carboxylates occurs in the *ortho* position (i.e. on the carbon atom β to the carboxyl), the potential magnitude of substitution effects is less than for aliphatics. Electron delocalization within the aromatic ring also tends to make the position of substitution less critical.

1.1.2. Effects of intramolecular H-bonding substituents on v_{as}

Intramolecular H-bonding between a carboxylate oxygen and a hydrogen in a nearby substituent will act to redistribute electron density within the carboxylate, breaking the

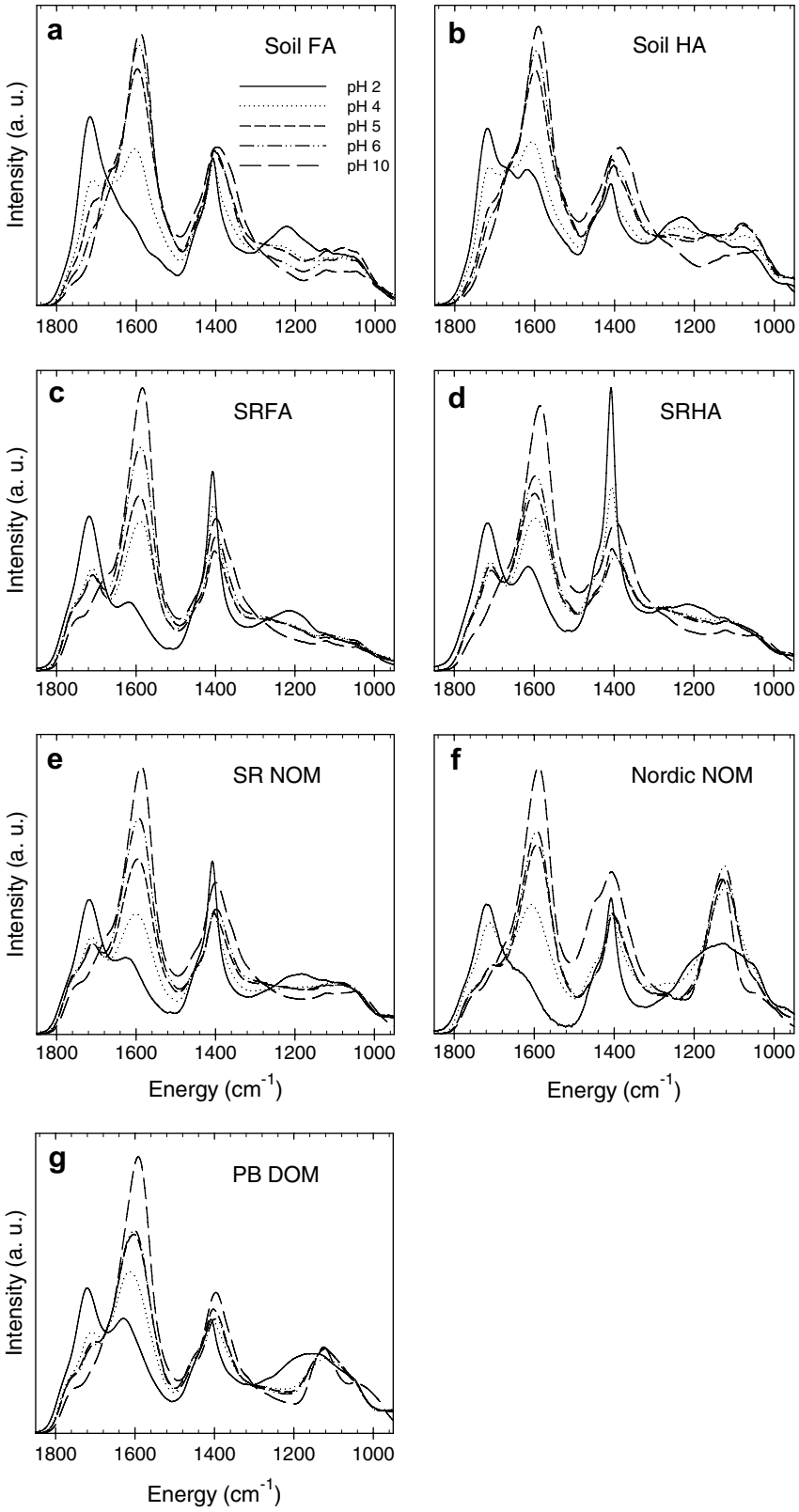

Fig. 4. ATR-FTIR spectra of humic substances at five pH values. (a) Elliot soil fulvic acid (soil FA), (b) Elliot soil humic acid (soil HA), (c) Suwannee River fulvic acid (SRFA), (d) Suwannee River humic acid (SRHA), (e) Suwannee River natural organic matter (SR NOM, reverse osmosis isolate), (f) Nordic reservoir natural organic matter (Nordic NOM, RO isolate), (g) Pine Barrens dissolved organic matter sample (PB DOM). Spectra at each pH have been roughly normalized to yield an isosbestic point at approximately 1670 cm^{-1}.

C—O bond symmetry and causing a shift in ν_{as} to higher energy. The magnitude of the shift depends on the H-bonding strength of the substituent and its proximity to the carboxylate (Figs. 2 and 3).

The H-bonding effect of a neighboring hydroxyl group is clearly observed in the aromatic acid *ortho*-hydroxybenzoate (salicylate), which exhibits a ν_{as} value 32 cm^{-1} higher than *para*-hydroxybenzoate. Though part of this difference may be due to inductive effects and vibrational coupling, the ν_{as} difference is significantly greater than those observed between other *ortho* vs. *para* substitutions (e.g., F, Cl, NO_2). Both the high ν_{as} energy and low pK_a of salicylate have been attributed to an H-bonding interaction between the carboxylate and the α-OH (Yost et al., 1990; Schwarzenbach et al., 2003). Additionally, the small-chain alkanedioic acids (oxalate through pimelate) exhibit higher ν_{as} values when only one of the two carboxyl groups is deprotonated, likely due to the strong H-bonding between protonated and deprotonated carboxyl groups. This effect is highly dependent on the distance between the two groups; note that both absolute magnitudes and the differences between ν_{as} values decrease with increasing chain length. Cyclopentane *trans*-1,2-dicarboxylic acid is most analogous to succinate (β-COO^-) and exhibits similar ν_{as} values.

Deuteration of the OH group weakens the H-bond interaction between OH and carboxylate. Yost et al. (1990) observed a shift in the ν_{as} of salicylate from 1572 to 1545 cm^{-1} upon deuteration of the phenolic OH. However, solvent H-bonding effects on ν_{as} (and ν_s) values introduced by the replacement of H_2O with D_2O appear to be minimal. Values for the ν_{as} and ν_s of benzoate in D_2O reported by Dunn and McDonald (1969) differ from other published H_2O values by 6 and 2 cm^{-1}, respectively, while Wojcik and Stock (1969) and Loring et al. (2000) observed similar vibrational frequencies for 2-pyridinecarboxylate (picolinate) in D_2O and H_2O, respectively (Fig. 3). Similarly, Strathmann and Myneni (2004) observed a slight increase in ν_{as} (<10 cm^{-1} for succinate, malonate, malate, and citrate) and no change in ν_s for aliphatic carboxylic acids in D_2O with respect to their H_2O values.

Positively charged amino groups also serve as excellent H-bond donors in organic molecules, such as amino acids. At pH values between 3 and 9 for most amino acids, the positively charged amine group interacts strongly with the deprotonated carboxyl group, resulting in ν_{as} values greater than 1600 cm^{-1}. On deprotonation of the amine at higher pH (>10), this value may decrease by 20–40 cm^{-1}, yet a significant degree of H-bonding still exists. The distance dependence in this case is illustrated by comparison of ν_{as} values for 2-, 3-, and 4-amino *n*-butyric acid (Fig. 2). As expected, ν_{as} is inversely correlated to the distance of the amino group from the carboxyl (Pearson and Slifkin, 1972).

1.1.3. Effects of metal coordination on ν_{as}

Metal complexation by the carboxylate causes ν_{as} to shift to a degree that depends on the nature of the complex formed. Many researchers use the observations of Deacon and Phillips (1980) as a first approximation (e.g., Persson et al., 1998, Quiles et al., 1999, and Strathmann and Myneni, 2004). Coordination with only one oxygen of the carboxylate (monodentate coordination) often causes an increase in ν_{as}, analogous to protonation of the carboxylate (Strathmann and Myneni, 2004). Conversely, bidentate chelation (coordination of a single metal by both oxygens of the carboxylate) and bidentate bridging (wherein each carboxylate oxygen is bound to separate metals) may result in a decrease in ν_{as}. These simple rules follow from the expected electron density shifts on coordination and hold for many solid-phase metal acetates (Deacon and Phillips, 1980), but their application to aqueous species is questionable (Strathmann and Myneni, 2004).

2. EXPERIMENTAL

2.1. Materials

Humic substance isolates, including Elliot soil humic and fulvic acid standards, Suwanee River humic acid reference, Suwanee River fulvic acid standard, and Nordic Reservoir and Suwanee River reverse osmosis isolate references, were obtained from the International Humic Substances Society (IHSS). These samples were used as obtained without further purification or isolation. High purity HCl, NaOH, and organic acids were obtained from Fisher and Sigma–Aldrich.

The Pine Barrens "leaf leachate" dissolved organic matter (DOM) sample was obtained from a secluded area of the Brendon T. Byrne State Forest (formerly known as the Lebanon State Forest) in the Pine Barrens of New Jersey, USA. The Pine Barrens comprises a topographically flat, mixed oak and pine forest region. The leachate sample was collected from a small open pool of water originating from rainwater runoff in the immediate vicinity and was stored without alteration in polypropylene bottles at 4 °C until use. The raw sample was filtered through a 0.1-μm polycarbonate disk prior to analysis.

2.2. Preparation of samples for ATR-FTIR spectroscopy

Stock solutions (500 mg/L) of the IHSS standards and references were prepared with deionized water (Milli-Q water, 18 MΩ resistivity), and their pH was adjusted to 10 with NaOH to ensure complete dissolution. Dilutions (1:10) were made from the stock solution and their pH readjusted to 10.0. The sample pH was then progressively lowered to pH 2.0 with HCl, while aliquots were removed at each 0.5–1 pH unit increment for the ATR-FTIR analysis, described below. For some samples, spectra were collected again as the pH was readjusted to 10, with aliquots collected for analysis at every 2 pH unit increment. This procedure was employed to ensure that there were no alterations in molecular structure induced by extreme pH adjustment. Significant differences were not observed between spectra collected before and after pH ramping (data not shown). Ionic strength effects were tested with the soil humic and soil fulvic acids by adding 0.5 M NaCl. Precipitation of the humic acid samples was not visibly observed at any pH values on the short timescale of the experiment, but centrifugation of the sample at pH 2 was sufficient to pull some of the humic acid out of solution, indicating that

the humic acid may have formed a colloidal suspension at low pH values. All samples were stirred vigorously while aliquots were removed for analysis.

Model carboxylic acids examined in this study were prepared in 100 mM concentrations or lower for aqueous infrared analyses. FTIR spectra were collected for pH values covering each of the dominant solution species (i.e., above, below, and between pK_a values). Ionic strength was not fixed directly, and varied slightly with pH adjustment. In some cases, thin film spectra (using the procedure described below) were also obtained for model compounds, using a solution concentration of 10 mM. Smaller solution concentrations were used in cases where solubility of the compound was limited.

To minimize carbonate interference in the infrared spectra, pH adjustments and sample preparations were performed in a glovebox purged with CO_2-free air obtained from a Parker Balston (Model 75-45-12VDC) FT-IR Purge Gas Generator. An Orion model 525A pH meter and Orion PerpHecT® ROSS® Model 8203 combination electrode were used for pH measurements.

2.3. ATR-FTIR spectroscopy

Mid-infrared ATR-FTIR spectra of NOM samples and select model carboxylic acids were collected on thin films, prepared by drying 250 μL aliquots of the samples on an attenuated total reflection (ATR) crystal. The samples were dried under a stream of dry, CO_2-free air (obtained from the Purge Gas Generator unit) until no bulk water was visibly present. In general, the NOM samples retained a thin, shiny, oily appearance after drying. The crystal was then immediately removed from airflow and placed in the FTIR sample chamber for analysis. For comparison, highly concentrated aqueous spectra of select samples were also collected. All infrared spectra were obtained in internal reflection mode with a Bruker IFS 66v/S spectrometer, using a Spectra-Tech ATR unit (A.R.K trough plate), a liquid nitrogen cooled mercury cadmium telluride (MCT) detector, and an aperture setting of 4 mm. Sample spectra were collected on zinc selenide (ZnSe) and AMTIR (selenium–arsenic–germanium glass) ATR crystals (45° incident beam angle, 12 reflections), housed in horizontal sampling troughs. The ZnSe crystal was used for sample pH values between 4 and 10, while the AMTIR was used for pH values lower than 4. Eight thousand scans (in two sets of 4000; approximately 10 min each) were collected and averaged for each sample using a Blackman–Harris 3-term apodization function within the OPUS-NT data collection software. A 4000-scan averaged spectrum was collected on the blank crystal immediately before and after each sample, and an equally weighted average of these two scans was used as the background.

2.4. Analysis of ATR-FTIR spectra

Initial processing of the background-normalized spectra included a linear baseline correction between 800 and 2000 cm^{-1}, followed by minor relative intensity scaling to yield an isosbestic point near 1670 cm^{-1}. To isolate the pH-dependent features in the IR spectra, subtractions were performed between spectra at high and low pH (e.g., pH 10 and 2, pH 6 and 4, etc.). This yielded curves with positive carboxylate anion features (ν_s and ν_{as}) and negative carboxylic acid features ($\nu_{C=O}$ and ν_{C-OH}). A series of Gaussian curves (maximum of 9) were used to fit the spectral features between 800 and 2000 cm^{-1} in the subtracted spectra. While each of the four carboxyl features could be fit using single Gaussian curves, additional curves were necessary to fit extraneous features, such as the water band near 1640 cm^{-1} (which remained after subtraction, varying unpredictably with pH), as well as the sharp, pH-dependent feature of unknown origin near 1407 cm^{-1}. The deconvolution was performed using the "Solver" routine in Microsoft Excel, based on minimization of the squared difference between data and fit values.

The deconvolution procedure proved useful in identifying the less obvious ν_s features and in obtaining accurate peak widths, which are potentially useful in assessing the degree of heterogeneity in carboxylic structural types. An additional concern was that the presence of a strong water feature at 1640 cm^{-1} would increase the apparent frequency of the ν_{as} band near 1600 cm^{-1}, thereby necessitating deconvolution. However, this effect proved to be minimal (differences between apparent and extracted ν_{as} were less than 5 cm^{-1}). Attempts were also made to quantify positions and widths of the ν_{C-OH} bands, but these peaks tended to be much broader and not as well defined; these values were not included in Table 1.

3. RESULTS AND DISCUSSION

The asymmetric and symmetric carboxylate stretching frequencies (ν_{as} and ν_s, respectively) of the NOM isolates are compared with the model carboxylate values to characterize the structural environments of carboxyl groups in NOM. Infrared spectroscopy is not sensitive enough to resolve each structural type present, but the method does allow for the broad classification of the dominant carboxyl structural types. Additionally, the infrared spectroscopy procedure probes all of the carboxyl groups in a given sample with equal weight. In the metal binding studies discussed above, only those carboxyl structures that are involved in coordinating the metal are probed. However, the sites involved in metal binding may vary depending on solution conditions, including metal type, pH, and relative metal:ligand concentrations, and may not accurately reflect the dominant carboxyl structures in a sample (Gregor et al., 1989b).

The air drying procedure used in the preparation of thin NOM films for infrared spectral collection also has its advantages. By using large, dilute sample volumes, pH adjustments could be made easily and accurately with minimal amounts of the NOM in solution. More importantly, the drying procedure proved to be a simple means of collecting clear, intense infrared spectra on the Pine Barrens DOM sample, without the need for potentially harmful extraction or concentration methods. Before discussing the results of the infrared absorption studies of NOM, however, it is necessary to investigate the impacts that the drying procedure may have had on the infrared spectra.

Table 1
Positions and peak widths of carboxyl group spectral contributions, determined through deconvolution

Sample	Position (cm^{-1})			Peak width (cm^{-1})		
	$\nu_{C=O}$	ν_{as}	ν_{s}	$\nu_{C=O}$	ν_{as}	ν_{s}
Elliot soil fulvic acid	1720	1589	1376	61	69	72
Elliot soil humic acid	1723	1587	1374	62	66	72
Suwanee River fulvic acid	1720	1585	1368	59	67	72
Suwanee River humic acid	1722	1586	1368	64	68	69
Suwanee River NOM	1720	1587	1370	59	70	70
Nordic Reservoir NOM	1720	1587	1375	60	70	56
Pine Barrens DOM	1722	1590	1382	58	67	55
Elliot soil humic acid (aqueous)	—	1577	1388	—	67	75

3.1. Effects of air-drying on infrared spectra

Infrared spectra were collected on the thin films after the samples became visibly dry, but retained a shiny, oily appearance. In successive scans, the second set collected showed a slight decrease in intensity in the 1620–1680 cm^{-1} and 2900–3600 cm^{-1} regions (data not shown), corresponding to the H—O—H bending and stretching modes of the water molecule, respectively. These slight decreases in signal intensity demonstrate that a small amount of residual water was present in the samples after drying, and the concentration of water progressively decreased on further desiccation in the dry air environment of the sample chamber. The hydrated state of the samples may suggest that the infrared spectra are more representative of aqueous-phase NOM, rather than NOM in solid form or in a KBr matrix (an important distinction, since we will be making comparisons between thin film NOM spectra and aqueous carboxylic acid spectra). To test this hypothesis, an aqueous spectrum of soil humic acid (3 g/L at pH 7) was collected for comparison with a thin film spectrum at the same pH (Fig. 5). Comparison of the raw spectra (Fig. 5a and b) illustrates that the spectral feature near 1600 cm^{-1} is broader and relatively more intense in the thin-film spectrum, due to the presence of residual water in the sample. Since the aqueous sample was collected against a water spectrum as background, bulk water features were effectively subtracted in the aqueous spectrum. After subtraction of the water feature from the thin-film spectrum, the aqueous and dried thin-film NOM spectra look very similar, but with ν_{as} shifted 10 cm^{-1} to higher energy in the latter, likely the result of a loss of hydration water and increased salt interaction (Cabaniss and McVey, 1995). Though the shift appears to be minimal, an allowance of this magnitude must be included when comparing our results with aqueous data reported in the literature. In the comparisons below (Section 3.3), the NOM ν_{as} values are all shifted uniformly by -10 cm^{-1} to account for air drying effects. This correction may be a slight underestimate for some samples, based on the ν_{as} value of 1565 cm^{-1} recently obtained by Yoon et al. (2004, 2005) for aqueous Suwannee river fulvic acid. However, uncertainty in the correction of 10 cm^{-1} or less does not significantly affect the interpretation given below. Further deconvolution revealed that the peak width of the ν_{as} contribution did not change significantly on drying.

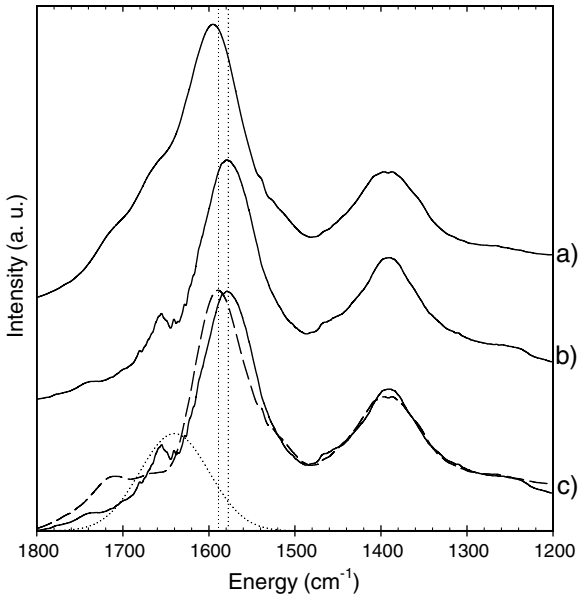

Fig. 5. ATR-FTIR spectra of aqueous and dried IHSS soil humic acid. (a) 250 mg/L soil humic acid sample dried as a thin film on the ATR crystal, pH 7. (b) Aqueous soil humic acid 3000 mg/L, pH 7. (c) A Gaussian profile centered at 1640 cm^{-1} with a halfwidth of 95 cm^{-1} representing the water HOH bend (dotted line) has been subtracted from the dried scan in (a), producing the dashed line spectrum. Comparison with the aqueous scan from (b) (solid line in (c)) demonstrates an approximately 10 cm^{-1} difference in asymmetric peak frequency.

To study the potential effects of drying on the individual carboxyl components in NOM, aqueous and dried spectra were also collected for several smaller carboxylic acids, including benzoate, glucuronate, malonate, lactate, pentenoate, polyacrylate, and the amino acids leucine and serine. Consistent with the NOM results, most of these compounds exhibited a shifting of ν_{as} to higher energies on drying, from as little as 3 cm^{-1} (benzoate, malonate) to as much as 15 cm^{-1} (pentenoate, polyacrylate). Behavior of the amino acids, however, was more complicated. These structures exhibited a splitting of the ν_{as} band, with the primary component shifting to lower energy in the thin films, possibly indicating a weaker interaction with the positively charged amine. The width of the ν_{as} peaks varied less predictably on drying. Lactate and pentenoate did not exhibit any change;

polyacrylate, malonate, and glucuronate values became wider (by 10, 25, and 29 cm^{-1}, respectively); and ν_{as} for benzoate became narrower by 4 cm^{-1} on drying. It is perhaps not surprising that no net change in peak width was observed for the soil humic acid after drying.

Drying the samples in this manner also alters pH and ionic strength. In the absence of buffering, pH would tend toward extremes with removal of water; values above pH 7 would increase, while values below pH 7 would decrease (a solution at pH 7 is expected to remain at 7 on drying, as the solution contains equal proportions of H^+ and OH^-). In our samples, carboxyl groups would buffer values just below 7. Based on the carboxylic concentration range of 7.14–15.24 mequ/g C reported by Ritchie and Perdue (2003) for a wide variety of IHSS humic and fulvic acids, we estimate carboxyl concentrations in the original 50 mg/L solutions to be between 1.8 and 3.8×10^{-4} mol/L, suggesting that the solution would strongly buffer pH changes for initial solution pH values between 4 and 7. Ultimately, however, the pH of the sample within the films is unknown, and no quantitative inferences regarding sample pK_a based on infrared spectra and initial solution pH can be made.

Effects of added salt on the dried spectra were tested on the soil humic and fulvic acid samples by rerunning these samples with 0.5 M NaCl. Differences between these spectra and those for the salt-free films included a small shift in ν_{as} and a slight difference in protonation behavior (data not shown). Shifts in ν_{as} were typically 5 cm^{-1} to lower energy with added salt, suggesting that the salt made the films more hygroscopic. Above pH 4, deprotonation was enhanced by the presence of salt, indicated by a decrease in intensity of the carboxylic acid features relative to the salt-free film at the same pH. While the effect was very small, it is consistent with the expected electrostatic screening of the carboxyl–proton interactions by the salt.

3.2. Infrared carboxylate features in NOM

The ATR-FTIR spectra of all NOM samples are qualitatively similar and are dominated by carboxylic spectral features. All samples exhibit a sharp ν_{as} band between 1585 and 1590 cm^{-1} (Fig. 4 and Table 1), a range that is strikingly narrow when compared to the range of values observed for model carboxylates (Figs. 2–4). This seems to suggest that the carboxylic structures are similar in all NOM samples studied, regardless of differences in their chemical fraction (humic vs. fulvic), origin (soil vs. fluvial), and the regional climate of their source. Additionally, the Pine Barrens DOM sample lies within this narrow range, despite the absence of any chemical purification (e.g., removal of chelating metals and "non-humic" biopolymers). This suggests that the majority of the carboxyls in this sample are either free or complexed by weakly binding metals. The $\nu_{C=O}$ of the protonated carboxyls varied within an equally narrow range of 1720–1723 cm^{-1} (Fig. 4).

Variation in the types of carboxylic structures in the sample may be evident as a broadening of the absorption bands, reflecting a sum of individual contributions differing from each other slightly in absorption frequency. Cabaniss et al. (1998) observed that the ν_{as} peak widths for model aliphatic dicarboxylic acids ranged between 42 and 60 cm^{-1}, which serves as a useful baseline for assessing peak broadening in a mixture due to heterogeneity. We assume that this range is also applicable to the aliphatic monocarboxylates, since Pike et al. (1993) found that the molar absorptivities for mono- and dicarboxylic acids do not differ significantly. The ν_{as} peak widths for the carboxylic acids studied herein (Section 3.1) are also within this range. The ν_{as} peak widths in the infrared spectra of the NOM samples varied between 66 and 70 cm^{-1}, suggesting that broadening due to variations in the carboxyl structure amounts to approximately 15 cm^{-1}. This heterogeneity factor is represented in Figs. 2 and 3 by the light gray bars that extend the darker bars by 8 cm^{-1} on either side. These lighter regions highlight structures that may potentially contribute to the main ν_{as} peak. Since the range of ν_s peak widths for organic acids is not as well known, the lighter gray bars in the ν_s figures were given the same 8 cm^{-1} width.

The spectral area in the subtractions at energies just below the main ν_{as} contribution required an additional, broader Gaussian curve in the deconvolution just below 1540 cm^{-1}. The peak area of this profile also increased with increasing pH to varying degrees in the NOM samples (typically 10–20%, but as much as 45% relative to the main peak). This area change at lower energy suggests that carboxylic contributions may be present between 1540 and 1580 cm^{-1} that are not captured by the narrower primary ν_{as} profile. Relative distributions of carboxylic structural types cannot be determined quantitatively with this information, since the broader profile is more sensitive to baseline drifts with pH and to the presence of other acidic groups such as $-NH_3^+$. In addition, variations in the area of this profile may also be affected by the lineshape of the primary ν_{as} peak (i.e., deviation from the Gaussian lineshape assumed in the deconvolution). Based on these observed spectral variations, and since all carboxyl groups have similar molar absorptivities, we believe that carboxylic groups with lower ν_{as} values are also present in NOM, but are in the minority.

The pK_a range of the dominant carboxyl structures in the NOM samples can be roughly approximated using the relation between pK_a and ν_{as} determined by Cabaniss and McVey (1995), based on a best-fit to experimental values obtained for non-halogen monocarboxylates:

$$pK_a = 63.41 - 0.03803\nu_{as} \quad (1)$$

The ν_{as} range of 1574–1582 cm^{-1}, obtained after applying the 10 cm^{-1} correction for drying effects, yields a pK_a range of 3.3–3.5. This range is slightly lower than the mean pK_a values of 3.8 ± 0.1 and 4.4 ± 0.1 for the IHSS fulvic and humic acids, respectively, based on pH titration results (Ritchie and Perdue, 2003). However, the averages based on pH titration also contain contributions from the carboxylates with lower ν_{as} values, which we believe are in the minority. This may account for part of the discrepancy, in addition to the macromolecular charge-screening effects.

Carboxylate symmetric stretching frequencies (ν_s) of the NOM samples ranged between 1368 and 1382 cm^{-1}. Identification of the ν_s was complicated in many samples by the

presence of the sharp feature at 1407 cm^{-1}. This feature increases with decreasing pH, exhibiting a strong pH trend that opposes that of the ν_s. Although this feature is apparent in all samples to varying degrees, it is strongest in the Suwannee River humic acid. The sharpness of the feature suggests that it may be an aromatic ring vibration, though it is not clear why it would exhibit a pH trend. Given this complicating factor, in addition to the vibrational coupling issues discussed above, ν_s is not as useful an indicator of structural environment as ν_{as}.

Features between 1700 and 1800 cm^{-1} present at high pH are likely due to carbonyl groups, such as carboxylic acid esters. While these appear to be in much lower concentration, the molar absorptivity of a carbonyl group is less than for a carboxylate. To quantify this, we performed aqueous IR measurements on a carboxylic acid and carboxylic acid ester solution mixture (ethyl 3-hydroxybutyrate + acetate), as well as a compound containing both a carboxylic acid and an ester (mono-ethyl succinate). Both spectra indicate that the spectral area of the carbonyl stretch near 1710 cm^{-1} is approximately 33% as large as the area of the ν_{as} feature of the carboxylate anion, suggesting that these structures may also be present in significant quantities. Additionally, residual features near 1550 and 1610 cm^{-1} in the pH 2.0 spectra may be from amide groups (Bellamy, 1980).

3.3. Nature of carboxyl groups in humic substances

Since the range of ν_{as} values for all examined NOM samples is narrow (1585–1590 cm^{-1}), a single comparison was made for all samples as a group. The gray bars have been added to Figs. 2 and 3, which reflect the range of infrared carboxylate absorption peaks observed for these samples. The dark gray bars in the charts represent the full range of values reported in Table 1, with a -10 cm^{-1} correction applied to the ν_{as} range to account for drying effects (see Section 3.1). The light gray bars extend this range by ± 8 cm^{-1} to account for uncertainty and structural variation. The predominant carboxylic structural types in the NOM samples were inferred based on the degree of overlap between the shaded regions and the energies of model organic acids.

Comparisons of ν_{as} positions of carboxylate groups in NOM with those of model carboxylates given in Figs. 2 and 3 suggest a predominance of α-substituted aliphatic carboxylates in the NOM isolates. With the exception of salicylate and furancarboxylate, the ν_{as} peaks for the substituted aromatic carboxylates expected in NOM (e.g., oxygen and carboxyl substituted structures) occur below 1570 cm^{-1}, while aliphatic carboxylates lacking α-substitution exhibit ν_{as} bands below 1560 cm^{-1}. Changes in spectral area with pH observed between 1540 and 1580 cm^{-1} could also indicate the presence of aromatic carboxylates and aliphatic carboxylates lacking α-substitution, present in lower concentrations.

The likelihood of specific substitutions may be assessed in terms of what is known regarding elemental composition and the relative distributions of oxygen functional groups in NOM. Humic and fulvic acids have average oxygen contents of approximately 35% and 45% by weight, respectively, compared to average nitrogen contents of less than 4%, and sulfur contents of approximately 1% (Steelink, 1985). Of the oxygen in humic substances, between 35% and 50% (humic acids) or between 40% and 75% (fulvic acids) may occur in the form of carboxylates (Stevenson, 1994; references therein). Given the high concentration of carboxyl groups compared to nitrogen and sulfur functional groups, we believe that the majority of the electron-withdrawing α-substitution necessary to achieve the high ν_{as} values may be in the form of other oxygen functional groups.

Of the oxygen-substituted monocarboxylates, the aliphatic acids D-lactate (α-hydroxy), gluconate (α, β-hydroxy), methoxyacetate (α-ether), and acetoxyacetate (α-ester), and the aromatic acids salicylate (2-hydroxy), 2- and 3-furancarboxylate, and tetrahydrofuran tetracarboxylate (*O*-heterocyclic) show particularly good overlap. (2- and 3-furan carboxylate actually exhibit split ν_{as} bands, with only one peak exhibiting strong overlap. They are probably not in the majority themselves, but may still be major contributors.) Several di- and poly-carboxylates also show strong overlap, most notably malonate and its alkane-substituted derivatives (below the 2nd pK_a), and diglycolate (also α-ether; see Fig. 6 for structures). Though succinate and tricarballylate do not exhibit strong overlap, their α-OH substituted analogues do (malate and citrate, respectively, in which the OH is α with respect to one carboxyl group in each structure). These results indicate that carboxyl groups with α-substitution of hydroxyl, ether/ester, and carboxyl groups (i.e., neighboring carboxyl groups attached to the same C atom) may be dominant structures in NOM. Similar substituents, when moved only as far as the β position, become insufficient to explain the high NOM ν_{as} range observed (e.g., 3-hydroxybutanoate, succinate, tricarballylate, and polyacrylate). Additionally, not all α-substitutions yield ν_{as} values near the NOM range; α-keto acids (glyoxalate, pyruvate) exhibit ν_{as} above this range, while the presence of a double-bond on the α-C yields values much lower than this range (pentenoate, maleate, fumarate). Finally, since the NOM does not exhibit the downward shift in ν_{as} at high pH exhibited by the di-acids, it is possible that α-OH and α-ether substitution are relatively more abundant than α-COOH. This result is in contrast to the studies by Yoon et al. (2004, 2005), who did observe a downward shift in ν_{as} above pH 4 for aqueous Suwannee River fulvic acid and Pahokee peat humic acid, which was attributed to the deprotonation of neighboring carboxyls. The ν_{as} results are therefore in agreement with the previous studies that suggested the presence of malonate-type structures (Gregor et al., 1989a,b), substituted succinates (Leenheer et al., 1998), and α-ester/ether substituted acids (Leenheer et al., 1995b). In addition, our studies extend these results to a broader variety of NOM isolates, including humic and fulvic acids from different climates and sources.

If these types of carboxyl groups are representative carboxyl structural environments in NOM, they must have points from which they may bind to larger molecules without dramatically affecting ν_{as}. For example, both glycolate

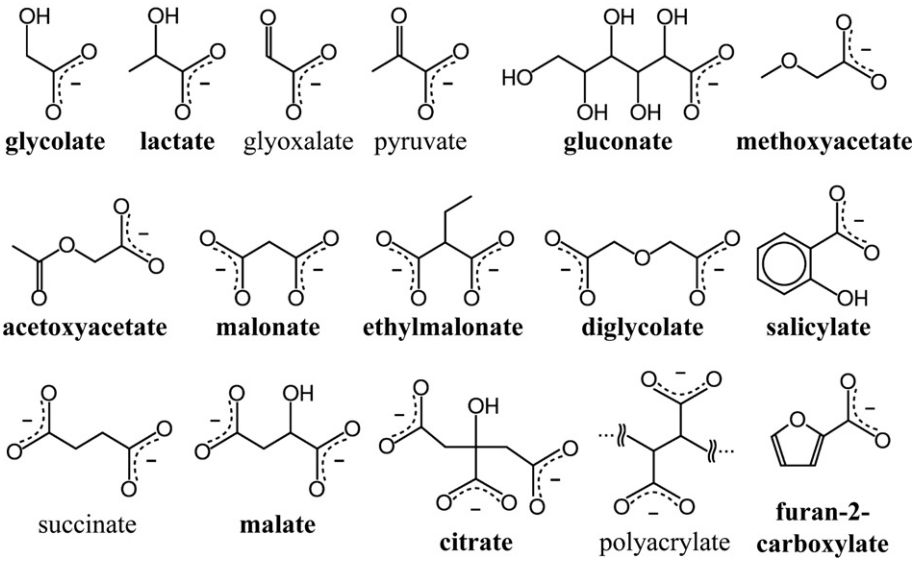

Fig. 6. Structures of the polycarboxylates and *O*-substituted monocarboxylates discussed in the text. Compounds in bold exhibit overlap in ν_{as} with the NOM samples.

and lactate exhibit overlap with the NOM ν_{as} range, but the methyl group on lactate serves as a point of attachment to some larger molecule, making it a more plausible structure (Fig. 6). It is encouraging that alkyl-substitution on malonate, providing the continuing side-chain for attachment, does not significantly alter ν_{as}; this is likely true for the hydroxyl-substituted succinate (malate) as well. Aromatic substitution, however, appears to be more complicated. The ν_{as} of salicylate is close to the NOM range, but ν_{as} drops out of range when the methyl group is added (5-methylsalicylate). The ν_{as} of salicylate also decreases when an OH is added in the *para* position (2,4-dihydroxybenzoate), suggesting that the ν_{as} for a salicylate-type structure in NOM will be highly dependent on how the structure is attached to the remainder of the molecule.

In contrast, the ν_s NOM range exhibits a high degree of overlap with many of the aromatic carboxylate values, including phalate, salicylate, 5-methylsalicylate, *p*-hydroxybenzoate, 2-and 3-furancarboxylate, and 2-pyrrolecarboxylate. Overlap with the aliphatic acid values is much less, with the exception of the substituted malonic acids. It is possible that since the ν_s of the aromatic acids fall within a more narrow range, it is these structures that give rise to the observed ν_s peak, despite being numerically less dominant based on the ν_{as} results. Given the complicating factors associated with the ν_s peak (greater sensitivity to vibrational coupling, interfering band at 1407 cm^{-1}), ν_{as} is assumed to be the better indicator of dominant carboxyl structures.

In part 2 of this series (Deshmukh et al., 2007), the carboxyl structural environments in soil and fluvial humic and fulvic acids were inferred using multidimensional NMR spectroscopy. Heteronuclear multiple bond correlation (HMBC) NMR was used to observe correlations between carboxylic ^{13}C and ^{1}H on C atoms α and β to the carboxyl. This method was able to detect α and β substituted aliphatic acids, 5-membered ring heterocyclic aromatic acids such as furancarboxylic acid, and 6-membered ring benzoic acid and heterocyclic aromatic acids. Many of the compounds suggested were similar to the structures inferred from infrared spectroscopy, including α-O- and α-COOH-substituted aliphatics, 2- and 3-furancarboxylate, and salicylate, providing further evidence for the presence of these structures. Moreover, differences among these structures were better resolved in the HMBC study. In particular, only one of the four samples (Suwannee River HA) exhibited a significant amount of benzoate-type aromatic acids (presumably salicylate), indicating that substituted benzoates, though consistent with the infrared results, may not be dominant in general. The primary signal in the HMBC results, however, derives from a mixture of unsubstituted aliphatic acids and/or α-substituted (particularly α-OH) aliphatic acids lacking protons on the α-carbon, such as α-substituted alicyclic carboxylic acids. The latter is consistent with the IR results, assuming that many of the α-substituted acid structures are fully substituted or are located midway along an aliphatic chain. Additionally, much of the unsubstituted aliphatic acid signal in the HMBC spectra may be due to aliphatic esters, which are difficult to distinguish using NMR spectroscopy. These structures are resolved in the IR spectra, and are shown to be present in small quantities.

4. CONCLUSIONS

The energy of the asymmetric stretching mode of the carboxylate in organic acids, determined using infrared spectroscopy, is a direct indicator of the structural environment of the carboxyl group. Using this information, the predominant molecular configurations of carboxyl groups in a variety of NOM samples were inferred. Little sample to sample variation was observed in the carboxylate ν_{as} region of the IR spectra, suggesting that all NOM isolates examined likely contain similar carboxyl structures, regardless of sample source and isolation technique. It was found that the

majority of the carboxyl groups in these samples are likely attached to aliphatic chains with oxygen substitution on the methylene groups α to the carboxyl. Representative models, based on overlap of the carboxylate asymmetric stretching bands, include short-chain monoacids with hydroxyl and ether or ester substitutions, as well as small, substituted di-acids (malonic and substituted succinic types). It is presumed that these types of structures would be connected to the larger humic and fulvic acids through an aliphatic side-chain. These structures are in agreement with other aliphatic structures proposed in the literature, and in particular, reaffirm the more general hypothesis that the majority of carboxyl structures are closely spaced and/or highly substituted. Of the aromatic acids included in the comparison, only furan-carboxylate and salicylate-type compounds exhibited ν_{as} values in the same range as NOM. Phthalate, an aromatic acid structure commonly assumed to be present in NOM in large quantities, does not exhibit strong overlap. Relative concentrations of COOH-substituted (neighboring carboxyl groups) and OH/ether-substituted groups could not be inferred precisely, but the COOH substitutions might be less abundant, since the ν_{as} peaks did not exhibit a downward shift at high pH for NOM (expected with deprotonation of the 2nd carboxyl). Though no discrete peaks were observed below the main ν_{as} features in the NOM samples, changes in spectral area with pH between 1500 and 1600 cm^{-1} (not accounted for by the Gaussian fit to the main ν_{as} peak) suggest that other aromatic acids and aliphatic acids lacking α-substitution likely make up a small, yet significant fraction of the carboxyl structures.

In addition, the procedure of drying aqueous samples to thin films on the ATR crystal proved to be a useful method for obtaining very clean, intense spectra from dilute aqueous samples. This method is particularly useful in analyzing raw, dilute DOM samples quickly and directly, without employing potentially harmful methods used to isolate or concentrate the samples. Since the thin-films still contained small amounts of water, the spectra are more representative of aqueous samples than of solid organic salts, though the small spectral changes observed were consistent with effects expected with drying.

ACKNOWLEDGMENTS

This research is funded by grants from NSF (Chemical Sciences-EMSI program), and from the BES, DOE (Geosciences). The authors thank A. Deshmukh and A. Leri for providing helpful comments on the manuscript. M.B.H. also gratefully acknowledges financial support from the EPA STAR and NSF graduate research fellowships.

REFERENCES

Barth A. (2000) The infrared absorption of amino acid side chains. *Prog. Biophys. Mol. Biol.* **74**, 141–173.

Bellamy L. J. (1980) *The Infrared Spectra of Complex Molecules*. Chapman and Hall, New York.

Cabaniss S. E. (1991) Carboxylic acid content of a fulvic acid determined by potentiometry and aqueous Fourier-transform infrared spectrometry. *Anal. Chim. Acta* **255**, 23–30.

Cabaniss S. E., Leenheer J. A., and McVey I. F. (1998) Aqueous infrared carboxylate absorbances: aliphatic di-acids. *Spectrochim. Acta A* **54**, 449–458.

Cabaniss S. E., and McVey I. F. (1995) Aqueous infrared carboxylate absorbances: aliphatic monocarboxylates. *Spectrochim. Acta A* **51**, 2385–2395.

Celi L., Schnitzer M., and Negre M. (1997) Analysis of carboxyl groups in soil humic acids by a wet chemical method, Fourier-transform infrared spectrophotometry, and solution-state carbon-13 nuclear magnetic resonance: a comparative study. *Soil Sci.* **162**, 189–197.

Crawford R. L. (1981) *Lignin Biodegradation and Transformation*. John Wiley and Sons, New York.

Deacon G. B., and Phillips R. J. (1980) Relationships between the carbon–oxygen stretching frequencies of carboxylato complexes and the type of carboxylate coordination. *Coord. Chem. Rev.* **33**, 227–250.

Deshmukh A. P., Pacheco C., Hay M. B., and Myneni S. C. B. (2007) Structural environments of carboxyl groups in natural organic molecules from terrestrial systems. Part 2: 2D NMR spectroscopy. *Geochim. Cosmochim. Acta.* **71**, 3533–3544.

Dobson K. D., and McQuillan A. J. (1999) In situ infrared spectroscopic analysis of the adsorption of aliphatic carboxylic acids to TiO_2, ZrO_2, Al_2O_3, and Ta_2O_5 from aqueous solutions. *Spectrochim. Acta A* **55**, 1395–1405.

Dobson K. D., and McQuillan A. J. (2000) In situ infrared spectroscopic analysis of the adsorption of aromatic carboxylic acids to TiO_2, ZrO_2, Al_2O_3, and Ta_2O_5 from aqueous solutions. *Spectrochim. Acta A* **56**, 557–565.

Dunn G. E., and McDonald R. S. (1969) Infrared spectra of aqueous sodium benzoates and salicylates in the carboxyl-stretching region: chelation in aqueous sodium salicylates. *Can. J. Chem.* **47**, 4577–4588.

Dupuy N., and Douay F. (2001) Infrared and chemometrics study of the interaction between heavy metals and organic matter in soils. *Spectrochim. Acta A* **57**, 1037–1047.

Gamble D. S., Schnitze M., and Hoffman I. (1970) Cu^{2+}-fulvic acid chelation equilibrium in 0.1 M KCl at 25.0 °C. *Can. J. Chem.* **48**, 3197–3204.

Goulden J. D. S., and Scott J. E. (1968) Infrared frequency and dissociation constant of the carboxylate group. *Nature* **220**, 698–699.

Gregor J. E., Powell H. K. J., and Town R. M. (1989a) Evidence for aliphatic mixed-mode coordination in copper(II)–fulvic acid complexes. *J. Soil Sci.* **40**, 661–673.

Gregor J. E., Powell H. K. J., and Town R. M. (1989b) Metal–fulvic acid complexing: evidence supporting an aliphatic carboxylate mode of coordination. *Sci. Total Environ.* **81**, 597–606.

Hadzija O., and Spoljar B. (1995) Quantitative determination of carboxylate by infrared spectroscopy: application to humic acids. *Fresenius' J. Anal. Chem.* **351**, 692–693.

Humbert B., Alnot M., and Quiles F. (1998) Infrared and Raman spectroscopical studies of salicylic and salicylate derivatives in aqueous solution. *Spectrochim. Acta A* **54**, 465–476.

Katlafsky B., and Keller R. E. (1963) Attenuated total reflectance infrared analysis of aqueous solutions. *Anal. Chem.* **35**, 1665–1670.

Kubicki J. D., Itoh M. J., Schroeter L. M., and Apitz S. E. (1997) Bonding mechanisms of salicylic acid adsorbed onto illite clay: an ATR-FTIR and molecular orbital study. *Environ. Sci. Technol.* **31**, 1151–1156.

Kubicki J. D., Schroeter L. M., Itoh M. J., Nguyen B. N., and Apitz S. E. (1999) Attenuated total reflectance Fourier-transform

infrared spectroscopy of carboxylic acids adsorbed onto mineral surfaces. *Geochim. Cosmochim. Acta* **63**, 2709–2725.

Leenheer J. A., Brown G. K., MacCarthy P., and Cabaniss S. E. (1998) Models of metal binding structures in fulvic acid from the Suwannee River, Georgia. *Environ. Sci. Technol.* **32**, 2410–2416.

Leenheer J. A., Wershaw R. L., Brown G. K., and Reddy M. M. (2003) Characterization and diagenesis of strong acid carboxyl groups in humic substances. *Appl. Geochem.* **18**, 471–482.

Leenheer J. A., Wershaw R. L., and Reddy M. M. (1995a) Strong-acid, carboxyl-group structures in fulvic acid from the Suwannee River, Georgia. 1. Minor structures. *Environ. Sci. Technol.* **29**, 393–398.

Leenheer J. A., Wershaw R. L., and Reddy M. M. (1995b) Strong-acid, carboxyl-group structures in fulvic acid from the Suwannee River, Georgia. 2. Major structures. *Environ. Sci. Technol.* **29**, 399–405.

Linder P. W., and Murray K. (1987) Statistical determination of the molecular structure and the metal binding sites of fulvic acids. *Sci. Total Environ.* **64**, 149–161.

Loring J. S., Karlsson M., Fawcett W. R., and Casey W. H. (2000) Attenuated total reflection-Fourier-transform infrared and ^{27}Al-nuclear magnetic resonance investigation of speciation and complexation in aqueous Al(III)-picolinate solutions. *Geochim. Cosmochim. Acta* **64**, 4115–4129.

Loring J. S., Karlsson M., Fawcett W. R., and Casey W. H. (2001) Infrared spectra of phthalic acid, the hydrogen phthalate ion, and the phthalate ion in aqueous solution. *Spectrochim. Acta A* **57**, 1635–1642.

Murray K., and Linder P. W. (1983) Fulvic acids: structure and metal binding. I. A random molecular model. *J. Soil Sci.* **34**, 511–523.

Murray K., and Linder P. W. (1984) Fulvic acids: structure and metal binding. II. Predominant metal binding sites. *J. Soil Sci.* **35**, 217–222.

Olsztynska S., Komorowska M., Vrielynck L., and Dupuy N. (2001) Vibrational spectroscopic study of L-phenylalanine: effect of pH. *Appl. Spectrosc.* **55**, 901–907.

Pearson J. F., and Slifkin M. A. (1972) The infrared spectra of amino acids and dipeptides. *Spectrochim. Acta A* **28**, 2403–2417.

Persson P., Karlsson M., and Ohman L. O. (1998) Coordination of acetate to Al(III) in aqueous solution and at the water–aluminum hydroxide interface: a potentiometric and attenuated total reflectance FTIR study. *Geochim. Cosmochim. Acta* **62**, 3657–3668.

Pike P. R., Sworan P. A., and Cabaniss S. E. (1993) Quantitative aqueous attenuated total reflectance Fourier transform infrared spectroscopy. Part II. Integrated molar absorptivities of alkyl carboxylates. *Anal. Chim. Acta* **280**, 253–261.

Quiles F., Burneau A., and Gross N. (1999) Vibrational spectroscopic study of the complexation of mercury(II) by substituted acetates in aqueous solutions. *Appl. Spectrosc.* **53**, 1061–1070.

Rahmelow K., Hubner W., and Ackermann T. (1998) Infrared absorbances of protein side chains. *Anal. Biochem.* **257**, 1–11.

Reuter, J. H., Ghosal, M., Chian, E. S. K., and Giabbai, M. (1983) Oxidative degradation studies of aquatic humic substances. In *Aquatic and Terrestrial Humic Materials*, Chapter 5 (eds R. F. Christman and E. T. Gjessing). Ann Arbor Science, Ann Arbor, MI.

Ritchie J. D., and Perdue E. M. (2003) Proton-binding study of standard and reference fulvic acids, humic acids, and natural organic matter. *Geochim. Cosmochim. Acta* **67**, 85–96.

Roddick-Lanzilotta A. D., and McQuillan A. J. (2000) An in situ infrared spectroscopic study of glutamic acid and of aspartic acid adsorbed on TiO_2: implications for the biocompatibility of titanium. *J. Colloid Interf. Sci.* **227**, 48–54.

Roger J., Delarbre J. L., and Maury L. (2003) Vibrational and structural analysis of saturated aliphatic compounds. XI. Vibrational spectra of 3-methylglutaric acid and its alkaline salts. *J. Raman Spectrosc.* **34**, 57–67.

Schnitzer M. (1969) Reactions between fulvic acid, a soil humic compound, and inorganic soil constituents. *Soil Sci. Soc. Am. Proc.* **33**, 75–81.

Schnitzer M., and Skinner S. I. M. (1965) Organo-metallic interactions in soils: 4. Carboxyl and hydroxyl groups in organic matter and metal retention. *Soil Sci.* **99**, 278–284.

Schwarzenbach R. P., Gschwend P. M., and Imboden D. M. (2003) *Environmental Organic Chemistry*. John Wiley and Sons Inc., Hoboken, NJ.

Specht C. H., and Frimmel F. H. (2001) An in situ ATR-FTIR study on the adsorption of dicarboxylic acids onto kaolinite in aqueous suspensions. *Phys. Chem. Chem. Phys.* **3**, 5444–5449.

Spinner E. (1964) The vibration spectra of some substituted acetate ions. *J. Chem. Soc.*, 4217–4226.

Sposito G. (1989) *The Chemistry of Soils*. Oxford University Press, Oxford.

Steelink, C. (1985) Implications of elemental characteristics of humic substances. In *Humic Substances in Soil, Sediment, and Water: Geochemistry, Isolation, and Characterization* (eds G. R. Aiken, D. M. McKnight, R. L. Wershaw and P. MacCarthy). John Wiley and Sons, New York.

Stevenson F. J. (1994) *Humus Chemistry: Genesis, Composition, Reactions*. John Wiley and Sons, New York.

Strathmann T. J., and Myneni S. C. B. (2004) Speciation of aqueous Ni(II)-carboxylate and Ni(II)-fulvic acid solutions: combined ATR-FTIR and XAFS analysis. *Geochim. Cosmochim. Acta* **68**, 3441–3458.

Tejedor-Tejedor M. I., Yost E. C., and Anderson M. A. (1990) Characterization of benzoic and phenolic complexes at the goethite/aqueous solution interface using cylindrical internal reflection Fourier transform infrared spectroscopy. 1. Methodology. *Langmuir* **6**, 979–987.

Tejedor-Tejedor M. I., Yost E. C., and Anderson M. A. (1992) Characterization of benzoic and phenolic complexes at the goethite/ aqueous solution interface using cylindrical internal reflection Fourier transform infrared spectroscopy. 2. Bonding structures. *Langmuir* **8**, 525–533.

Thorn, K. A. (1989) Nuclear-magnetic-resonance spectrometry investigations of fulvic and humic acids from the Suwannee River. In *Humic Substances in the Suwannee River, Georgia: Interactions, Properties, and Proposed Structures* (eds R. C. Averett, J. A. Leenheer, D. M. McKnight, and K. A. Thorn). United States Geological Survey Open-File Report 87-557, Denver, CO, pp. 251–310.

Town R. M., and Powell H. K. J. (1993) Ion-selective electrode potentiometric studies on the complexation of copper(II) by soil-derived humic and fulvic acids. *Anal. Chim. Acta* **279**, 221–233.

Tunesi S., and Anderson M. A. (1992) Surface effects in photochemistry: an in situ cylindrical internal reflection-Fourier transform infrared investigation of the effect of ring substituents on chemisorption onto TiO_2 ceramic membranes. *Langmuir* **8**, 487–495.

Wagner G. H., and Stevenson F. J. (1965) Structural arrangement of functional groups in soil humic acid as revealed by infrared analysis. *Soil Sci. Soc. Am. Proc.* **29**, 43–48.

Wang F., and Berglund K. A. (2000) Monitoring pH swing crystallization of nicotinic acid by the use of attenuated total reflection Fourier transform infrared spectrometry. *Ind. Eng. Chem. Res.* **39**, 2101–2104.

Wershaw R. L., Leenheer J. A., Kennedy K. R., and Noyes T. I. (1996) Use of ^{13}C NMR and FTIR for elucidation of degradation pathways during natural litter decomposition and composting. 1. Early stage leaf degradation. *Soil Sci.* **161**, 667–679.

Wojcik J. F., and Stock T. H. (1969) Aqueous infrared studies of the pyridine carboxylic acids. *J. Phys. Chem.* **73**, 2153–2157.

Wood J. C., Moschopedis S. E., and Denhertog W. (1961) Studies in humic acid chemistry. 2. Humic anhydrides. *Fuel* **40**, 491–502.

Yoon T. H., Johnson S. B., and Brown G. E. (2004) Adsorption of Suwannee River fulvic acid on aluminum oxyhydroxide surfaces: An in situ ATR-FTIR study. *Langmuir* **20**, 5655–5658.

Yoon T. H., Johnson S. B., and Brown G. E. (2005) Adsorption of organic matter at mineral/water interfaces. IV. Adsorption of humic substances at boehmite/water interfaces and impact on boehmite dissolution. *Langmuir* **21**, 5002–5012.

Yost E. C., Tejedor-Tejedor M. I., and Anderson M. A. (1990) In situ CIR-FTIR characterization of salicylate complexes at the goethite/aqueous solution interface. *Environ. Sci. Technol* **24**, 822–828.

Associate editor: Carol Arnosti